Numerical study on the influence of mesomechanical properties on macroscopic fracture of concrete

W. C. Zhu†, C. A. Tang‡ and S. Y. Wang‡†

Laboratory of Numerical Test on Material Failure, School of Resource and Civil Engineering, Box 138, Northeastern University, Shenyang 110004, China

(Received March 24, 2004, Accepted December 28, 2004)

Abstract. The numerical simulations on the influence of mesoscopic structures on the macroscopic strength and fracture characteristics are carried out based on that the concrete is assumed to be a three-phase composite composed of matrix (mortar), aggregate and bond between them by using a numerical code named MFPA. The finite element program is employed as the basic stress analysis tool when the elastic damage mechanics is used to describe the constitutive law of meso-level element and the maximum tensile strain criterion and Mohr-Coulomb criterion are utilized as damage threshold. It can be found from the numerical results that the bond between matrix and aggregate has a significant effect on the macroscopic mechanical performance of concrete.

Key words: concrete; mesoscopic; fracture process; numerical simulation.

1. Introduction

The numerical simulation of the damage and fracture process of concrete material has evolved considerably in the past years. It has been generally accepted that the deformation and fracture of concrete under external loading is associated with very complicated progressive failure processes, which are characterized by initiation, propagation, and coalescence of microcracks. The difficulty in simulating the fracture behavior of concrete is dominantly related to the heterogeneities present in the medium. Traditionally, models for concrete have been based on one of the classical approaches such as elasticity, plasticity and viscoelasticity, but these macroscopic models do not consider the heterogeneity of concrete, and are not applicable to the mechanical behaviour of concrete over its full range of behaviour. Therefore, they are not successfully used in studying the effect of the internal heterogeneous structures on the fracture process of concrete.

As pointed out by Wittmann (1983), concrete is a typical multi-scale material with different structural details appearing at different levels of observation, the research of concrete material focused mainly on these three distinct levels, namely the micro-, meso- and macro-level. The different mechanical response that can be found in a material at a level (such as macroscopic level) can be explained in terms of the structural response at a low level (such as mesoscopic level) (Van

† Associate Professor (Ph.D.), Corresponding author, E-mail: wczhu@mail.edu.cn
‡ Professor (Ph.D.)
‡† Ph.D. Student

Mier 1997). The mesoscopic level was generally considered to be 10^{-3} m when we study the laboratory scale responses of concrete (Van Mier 1997). At the meso-level the concrete is heterogeneous and the big pores, pre-existing cracks and inclusions are introduced as the main characteristic features (Wittmann 1983).

In recent years, there has been a growing interest in the numerical modelling of the fracture process of concrete, which is important for engineering higher-performance concrete and for enhancing the capability of numerical methods for engineering applications. By contrast to the experimental investigation, the numerical simulation is flexible in studying the effect of mesoscopic mechanical properties on macroscopic mechanical response of concrete subjected to a variety of loading conditions.

The random particle model presented by Bažant *et al*. (1991), UDEC used by Vonk *et al*. (1991), the mechanical model proposed by Mohamed and Hansen (1999a, b), the lattice model used in the Stevin laboratory (Schangen and Van Mier 1992, Van Mier and Van Vliet 1999) and discontinuous deformation analysis (DDA) of Pearce *et al*. (2000) are all typical mesoscopic models that can simulate the fracture process of concrete by considering its meso-level heterogeneity. In these mesoscopic models, the lattice model (Schangen and Van Mier 1992) and mechanical model proposed by Mohamed and Hensen (1999a, b), are more successful in simulating the fracture characteristics of concrete under a lot of laboratory tests (such as uniaxial compression test, uniaxial tensile test and three-pint bending test) based on the assumption that tensile cracking at the meso level is the only failure mode associated with the macroscopic fracture of concrete materials. By including a shear-type damage threshold, the mesomechanical model proposed by authors was also effective in capturing the fracture characteristics and strength envelope of concrete and rock under uniaxial or biaxial loading conditions (Zhu *et al.* 2002, Tang 1997). In this investigation, the concrete is assumed to be a three-phase composite composed of the cement matrix phase, the aggregate phase and the matrix-aggregate bond phase, the effect of mechanical properties of each mesoscopic phase on the macroscopic numerical response of concrete is numerically studied.

2. Mesosmechanical model

In order to consider the heterogeneity of concrete at mesoscopic level, the concrete is assumed to be a three-phase composite composed of the cement matrix phase, the aggregate phase and the matrix-aggregate bond phase. The concrete is numerically described with many mesoscopic elements with same size, and the mechanical parameters of these mesoscopic elements in each phase are assumed to conform to specific Weibull distribution. The mesoscopic elements are also acted as elements for finite element analysis, which are assumed as homogeneous and isotropic. The fracture process simulation is attained when using finite element method (FEM) as the basic stress analysis tools, where the four-node isoparametric element is used as the basic element in the finite element mesh, and the elastic damage constitutive relationship of meso-level elements is incorporated.

2.1 Assignment of material properties

In order to reflect the heterogeneity of quasi-brittle materials at meso-level, the mechanical parameters of materials, including the Young's modulus and strength are assumed to conform to the Weibull distribution as defined in the following statistic density function:

$$f(u) = \frac{m}{u_0}\left(\frac{u}{u_0}\right)^{m-1} \exp\left(-\frac{u}{u_0}\right)^m \tag{1}$$

where u is the parameter of element (such as strength or elastic modulus); the scale parameter u_0 is related to the average of element parameter and the parameter m defines the shape of the distribution function. The parameter m defines the degree of material homogeneity, and is called a homogeneity index. According to the definition of Weibull distribution, the value of parameter m must be larger than 1.0. Fig. 1 is the specimens that are all composed of 100 × 100 elements, produced randomly by computer according to the Weibull distribution with different homogeneity indices. Here the specimen produced numerically with given distribution of material properties is called "numerical specimen". In Fig. 1 the different degree of grey scale color corresponds to different values of strength of elements. The stochastic distribution of strength of elements is also given in Fig. 2. It can be found that the strengths of more elements are distributed in a narrow range around u_0 with the higher values of homogeneity index. Therefore, the high value of homogeneity index leads to more homogeneous numerical specimens. In this investigation, it is assumed that

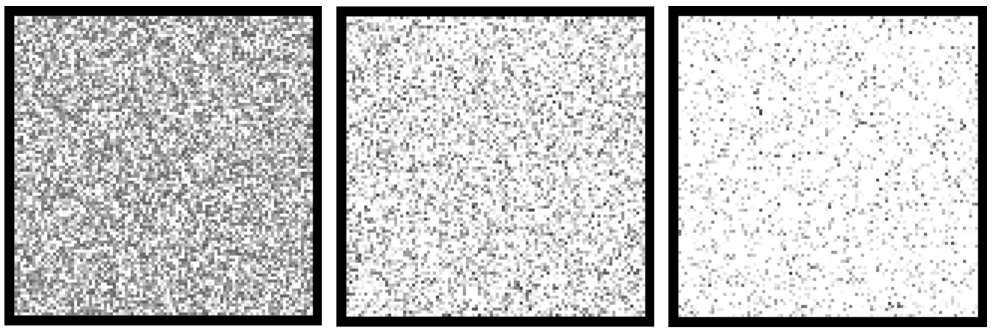

$m = 1.5$ $m = 3$ $m = 6$

Fig. 1 Distribution of strength of specimens with different homogeneity index (the gray degree in the figure denotes the magnitude of strength of elements)

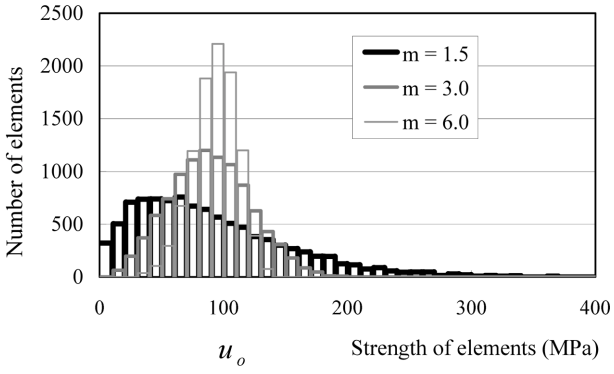

Fig. 2 Histogram of strength of elements in numerical specimen with different homogeneity index (The numerical specimen is shown in Fig. 1, which is composed of 10000 elements and the Weibull parameter u_0 is 100 MPa.)

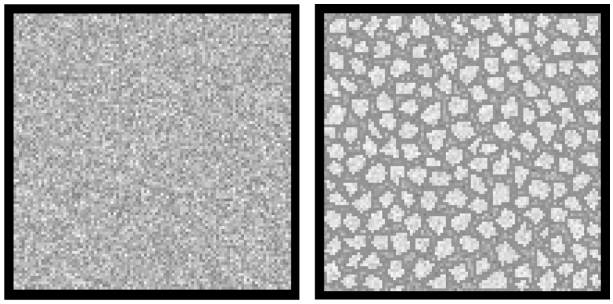

(a) Matrix specimen (b) Concrete specimen

Fig. 3 Distribution of elastic modulus of matrix and concrete (the gray degree in the figure denotes the magnitude of strength of elements)

Young's modulus and strength conform to two individual distributions with the same heterogeneity index. In previous paper (Zhu *et al*. 2002), how the homogeneity index affects the macroscopic mechanical response of numerical specimens has been discussed and it is found that the homogeneity index is an important parameter of Weibull distribution to control the macroscopic response of numerical specimen.

The numerical specimen is composed of rectangular elements with the same size, and different mechanical properties corresponding to their location in matrix, aggregate or bond phases. In our numerical model, no special interface elements are included to simulate the bond phase in concrete. The mechanical parameters of matrix are specified stochastically at first according to a Weibull distribution (as shown in Fig. 3a). Then the aggregates with given mechanical parameters can be placed on the numerical specimen to replace the matrix elements in the same location, and the system can automatically form bonds between matrices and aggregates with assigned bonds parameters (as shown in Fig. 3b). The elements in aggregate have the higher homogeneity index than those in matrix and bond. In this model, only the constitutive relationship of these meso-level elements is necessary to be given, and the mechanical properties of macroscopic concrete can be acquired by the sum of all the interactions of these mesoscopic elements after numerical analysis.

2.2 Constitutive relations of element

In the paper, the concrete material is analyzed at meso level. The stress-strain curve of the element is considered linear elastic till the given damage threshold is attained, and then is followed by softening. For simplicity, an elastic damage model with constant residual strength is used (Zhu *et al.* 2002). The maximum tensile strain criterion and Mohr-Coulomb criterion are selected as two damage thresholds. At any event, the tensile strain criterion is preferential. It has been proved elsewhere (Zhu *et al*. 2002) that the macroscopic mechanical response of concrete at macroscopic level can be simulated effectively by using this simple constitutive law.

In elastic damage mechanics, the elastic modulus of element may degrade gradually as damage progresses. The elastic modulus of damaged material is defined as follows.

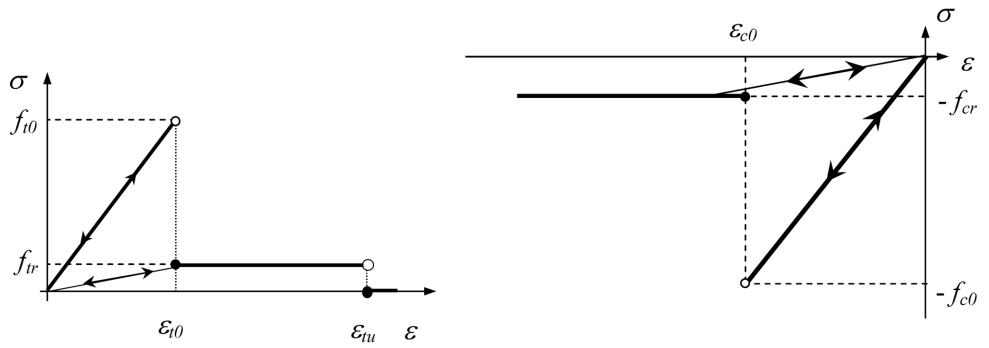

(a) Under uniaxial tension (b) Under uniaxial compression

Fig. 4 Elastic damage constitutive law of element under uniaxial stress conditions (f_{t0} and f_{tr} are uniaxial tensile strength and residual uniaxial tensile strength of element, respectively. f_{c0} and f_{cr} are uniaxial compressive strength and residual corresponding strength of element, respectively)

$$E = \begin{cases} (1-D^{+})E_0 & \text{for tensile damage} \\ (1-D^{-})E_0 & \text{for shear damage} \end{cases} \tag{2}$$

where D^+ and D^- represent the damage variable for tensile damage and shear damage, respectively. E and E_0 are elastic modulus of the damaged and the undamaged material, respectively. Here the element as well as its damage is assumed isotropic elastic, so the E, E_0 and D are all scalar. Through out this paper, tensile stress and strain are referred to as positive. No initial damage is incorporated in this model, at the beginning the stress-strain curve is linear elastic and no damage occurs, i.e., D^+ (or D^-) = 0.

When the mesoscopic element is under uniaxial tensile stress, the constitutive relationship that is elasto-brittle damage with given specific residual strength is shown in Fig. 4. When the maximum tensile strain criterion is met, the damage of element occurs. Herein this kind of damage is called tensile damage.

According to the constitutive relationship of mesoscopic element under uniaxial tension as shown in Fig. 4(a), the damage evolution of element can be expressed as

$$D^{+} = \begin{cases} 0 & \varepsilon < \varepsilon_{t0} \\ 1-\dfrac{\lambda\varepsilon_{t0}}{\varepsilon} & \varepsilon_{t0} \le \varepsilon < \varepsilon_{tu} \\ 1 & \varepsilon \ge \varepsilon_{tu} \end{cases} \tag{3}$$

where f_{t0} is the uniaxial tensile strength and λ is the residual strength coefficient that is defined by $f_{tr} = \lambda f_{t0}$ and f_{tr} is called residual tensile strength. ε_{t0} is the strain at the elastic limit, which is the so-called threshold strain. ε_{tu} is the ultimate tensile strain of the element, which indicates that the element would be completely damaged when the tensile strain of element attains this ultimate tensile strain. The ultimate tensile strain is defined as $\varepsilon_{tu} = \eta\varepsilon_{t0}$, where η is called ultimate strain coefficient.

Additionally, it is assumed that the damage of mesoscopic element in multiaxial stress field is also isotropic and elastic, and therefore the above-described constitutive law for uniaxial tensile stress can be extended to use for three-dimensional stress states. Under multiaxial stress states the element still damages in tensile mode when the combination of major tensile strain attains the above threshold strain ε_{t0}. The constitutive law of element subjected to multiaxial stresses can be easily obtained only by substituting the strain ε in Eq. (3), with equivalent strain $\bar{\varepsilon}$.

The equivalent strain $\bar{\varepsilon}$ is defined as follows.

$$\bar{\varepsilon} = \sqrt{\langle \varepsilon_1 \rangle^2 + \langle \varepsilon_2 \rangle^2 + \langle \varepsilon_3 \rangle^2} \tag{4}$$

where ε_1, ε_2 and ε_3 are principal strain, and < > is a function defined as follows:

$$\langle x \rangle = \begin{cases} x & x \geq 0 \\ 0 & x < 0 \end{cases} \tag{5}$$

It must be emphasized that when $D^+ = 1$, it can be calculated from Eq. (2) that the damaged elastic modulus is zero, which would make the system of equations ill-posed, therefore, in this model a relatively small number, i.e., 1.0e-05 is specified to the elastic modulus under this condition.

Mohr-Coulomb criterion as expressed follows is chosen to be the second damage threshold.

$$\frac{1 + \sin\phi}{1 - \sin\phi}\sigma_1 - \sigma_3 \geq f_{c0} \tag{6}$$

where σ_1 and σ_3 are major and minor principal stress respectively. f_{c0} is uniaxial compressive strength and ϕ is the internal friction angle. Again, compressive stresses are negative and tensile stresses are positive. This kind of damage is called shear damage because the stress conditions of element meet the Mohr-Coulomb criterion. A similar constitutive law to the tensile is given in Fig. 4(b) when the element is under uniaxial compression and damaged in shear mode when the Mohr-Coulomb criterion is met. The damage variable D^- can be described as follows.

$$D^- = \begin{cases} 0 & \varepsilon > \varepsilon_{c0} \\ 1 - \dfrac{\lambda \varepsilon_{c0}}{\varepsilon} & \varepsilon \leq \varepsilon_{c0} \end{cases} \tag{7}$$

where λ is also residual strength coefficient. It is assumed that $f_{cr}/f_{c0} = f_{tr}/f_{t0} = \lambda$ hold true when the mesoscopic element is under uniaxial compression or uniaxial tension.

When the element is under multi-axial stress state and satisfies the Mohr-Coulomb criterion, the shear damage occurs, and we must consider the effect of other principal stress in this model during damage evolution process. When the Mohr-Coulomb criterion is met, the minor principal strain (maximum compressive principal strain) ε_{c0} at the peak value of minor principal stress is calculated.

$$\varepsilon_{c0} = \frac{1}{E_0}\left[-f_{c0} + \frac{1 + \sin\phi}{1 - \sin\phi}\sigma_1 - \mu(\sigma_1 + \sigma_2)\right] \tag{8}$$

where μ is the Poisson's ratio.

In addition, it is assumed that the damage evolution is only related to the maximum compressive principal strain ε_3. Therefore, the maximum compressive principal strain ε_3 of damaged element is used to substitute the uniaxial compressive strain ε in Eq. (7). Thus, the former Eq. (7) can be

extended to biaxial or triaxial stress states.

$$D^{-} = \begin{cases} 0 & \varepsilon_3 > \varepsilon_{c0} \\ 1 - \dfrac{\lambda \varepsilon_{c0}}{\varepsilon_3} & \varepsilon_3 \le \varepsilon_{c0} \end{cases} \tag{9}$$

From the above derivation of damage variables D^{+} and D^{-}, which are generally called the damage evolution law in damage mechanics, as well as Eq. (2), the damaged elastic modulus of element at different stress or strain level can be calculated. Since the elastic damage model is used for elements, the unloaded element keeps its current elastic modulus and strength. That is to say, the element will unload elastically and no residual deformation is incorporated in the numerical model.

In a previous paper (Zhu *et al*. 2002), how the parameters such as the homogeneity index *m*, residual strength coefficient, and ultimate strain coefficient affect the macroscopic stress-strain response of numerical specimen had been discussed in detail. It proved that the effect of constitutive parameters is minor on the condition that the residual strength coefficient λ and ultimate strain coefficient η is in the range $0 < \lambda \le 0.1$ and $2 \le \eta \le 5$, respectively. However, the homogeneity index *m* is the most important parameter that affects the macroscopic response of macroscopic numerical specimen. The validation studies to some typical laboratory tests of concrete had been undertaken and proved that this model could effectively simulate the non-linearity of stress-strain response, localization of deformation, strain softening, and crack propagation process in concrete and rock under a variety of static loadings (Zhu *et al*. 2002).

The simulation of crack initiation and propagation in this investigation is just as the method used in smeared crack model, the crack is smeared over the whole element, which has the advantage of leaving untouched the mesh topology. No special singular element is adopted. When the stress state of an element meets the damage threshold, the element will damage in tensile or shear mode. Only when the maximum tensile strain of the damaged element attains a given ultimate tensile strain, the damaged element will become totally cracked. One of the main features of this kind of model is that there is no need for a pre-existing crack to simulate the crack initiation and propagation. The numerical model can simulate the initiation, propagation, and coalescence of multiple cracks effectively and easily.

The above model was fully implemented into a numerical code named MFPA (abbreviated from Material Failure Process Analysis) using Microsoft Visual C++ and Compaq Visual Fortran under Microsoft Windows 98/2K/XP. MFPA was validated extensively and had been successfully used to simulate the brittle failure process of concrete and rock subjected to a variety of static loading conditions (Zhu *et al.* 2002, Tang 1997).

3. Concrete specimen with one aggregate

For simplification, the concrete specimen with one aggregate as shown in Fig. 5, which was also experimented by Tan *et al*. (1995) in the past, is numerically studied. The bond phase is included around the circular aggregate in order to study the effect of its mechanical properties on macroscopic mechanical response of concrete specimen. This concrete specimen is discretized into 130 × 110 rectangular elements with the same size of 1 mm × 1 mm. In this section, the mechanical properties of matrix is fixed, and those of aggregate and bond phases are changed for

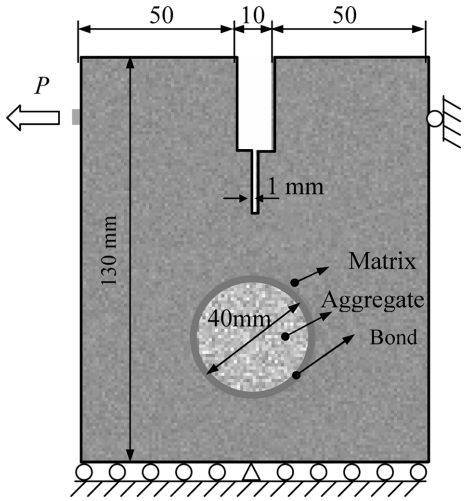

Fig. 5 The tensile specimen of concrete with one aggregate (the bond between aggregate and matrix is included.)

Table 1 Weibull distribution parameters of matrix and aggregates used in numerical study

Phase	Mean of Young's modulus (GPa)	Mean of uniaxial compressive strength (MPa)	Homogeneity index *m*
Matrix	27.3	165	3.0
Strong aggregate	80.0	500	6.0
Weak aggregate	15.0	80	6.0

every numerical specimens in order to predict their effect on mechanical response of concrete. The mechanical properties (including Young's modulus, strength, etc.) of three phases in concrete are assumed to be heterogeneous and specified according to the Weibull distribution with the parameters presented in Table 1.

It is important to mention that if a numerical specimen of matrix with a size of 100 mm × 100 mm is established when the mean strength of elements is specified to be 165 MPa, the global compressive strength as simulated with our model is only 30 MPa. Only when the homogeneity index tends to infinite (the specimen tends to be homogeneous) the numerically simulated strength would be close to the given mean strength of elements (Zhu *et al*. 2002). Because the failure initiates at element with the lower strength when the specimen is subjected external loading, and more detailed description about it has been given elsewhere (Zhu *et al*. 2002). This can explain why the average strengths given in Table 1 are much larger than those of real materials. However, the ratio between the global compressive strength of numerical specimen and mean strength of all elements are fixed for a given homogeneity index.

For each numerical specimen, a horizontal load is applied at left loading point step by step in displacement-controlled mode, and the corresponding point at the right side is prevented from movement in horizontal direction. The displacement is applied step by step, and the initial value and increment are both 0.001 mm.

3.1 Hard aggregate concrete

For hard aggregate concrete, it is assumed that the bond phase and matrix phase have the same homogeneity index, and the ratios of mechanical parameters (including Young's modulus, uniaxial compressive strength and uniaxial tensile strength) between bond and matrix phases, which is denoted with r are specified to be 0.4, 0.6, 0.8 and 1.0, respectively. From the numerical simulation, the load-displacement curves for four numerical specimens are obtained and shown in Fig. 6. Correspondingly, the cracking patterns at three different loading levels (those are at half peak load, peak load and final step) are shown in Fig. 7.

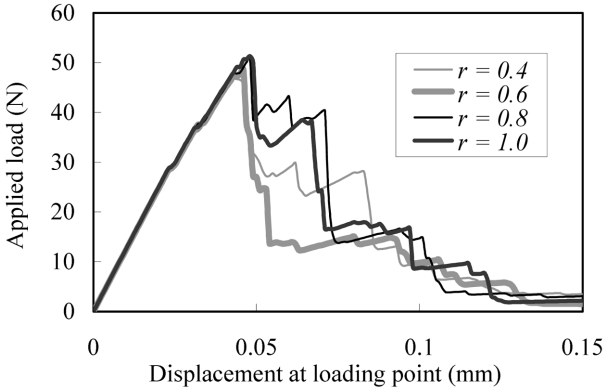

Fig. 6 Numerical results of the load-displacement curve at loading point for different specimens (r denotes the ratio of mechanical parameters between bond phase and matrix phase)

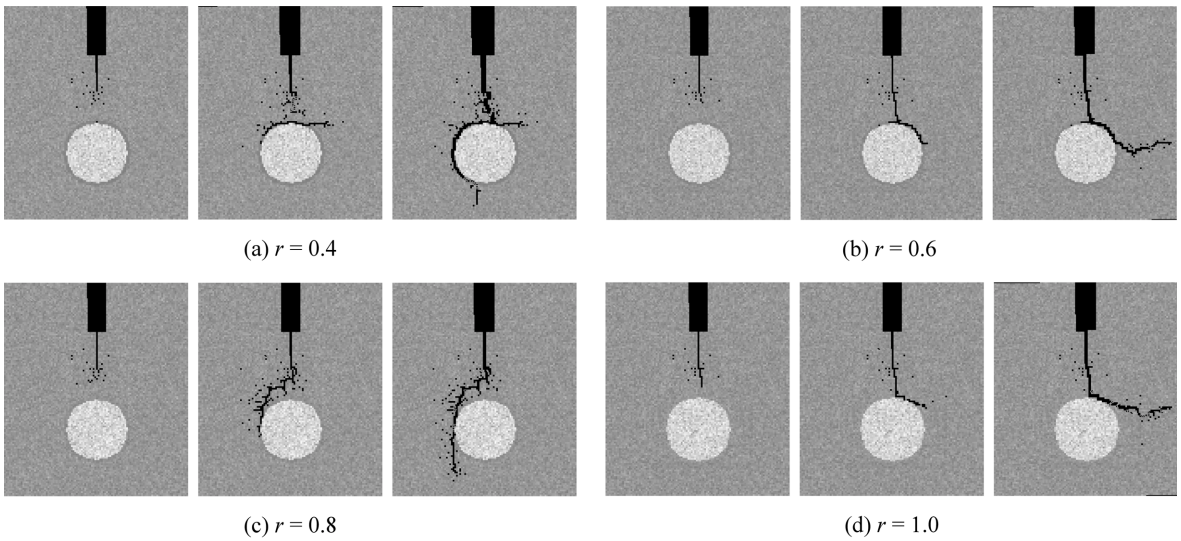

Fig. 7 Cracking patterns of strong aggregate concrete with different mechanical parameters of bond phase (The ratio of mechanical parameters between bond phase and matrix phase is denoted with r. For different values of r, the cracking patterns at peak loading, after-peak loading and final step are presented.)

With regard to the lowest bond mechanical parameters (r = 0.4), the crack propagates downwards, and simultaneously the new crack also initiates at the bond phase. At last these cracks coalesce to each other. With the increase of r (r = 0.6), the crack propagates downwards to the aggregates and grows continuously at the bond phase. When r = 0.8 and r = 1.0, the crack usually goes downwards, bypasses the bond and aggregate phase, and grows in matrix phase. By contrast, for the smaller r (r = 0.4 and 0.6) the peak loading of the specimen is relatively low (as shown in Fig. 6) because the aggregate doesn't lead to enhancing the strength of concrete specimen. It should be noted that the pre-existing crack propagates in different path before it attains the bond even if it will eventually go through the bond phase (for example, r = 0.4 and 0.6). This is because the stress conditions around the crack tip are changed due to the different heterogeneous mechanical properties are specified to the bond phase around the strong aggregate for each numerical specimen.

3.2 Weak aggregate concrete

As regards the weak aggregate concrete, the bond phase is assumed to have weak mechanical properties compared to aggregate. The fracture process of the numerical specimen when the ratios of mechanical parameters between bond and aggregate (r) are 0.4, 0.6, 0.8 and 1.0 is numerically studied, and the cracking pattern at the final loading step is shown in Fig. 8. Compared to the numerical results presented in Fig. 7, it can be seen that for smaller value of r (r = 0.4 and 0.6), the crack propagates downwards and grows at the bond phase. For the larger value of r (r = 0.8 and 1.0), the crack penetrates the weak aggregate, and the crack propagation path tends to be linear.

Therefore, it can be concluded that the bond between aggregate and matrix in normal weight concrete and lightweight concrete plays an important role in the crack propagation and strength of concrete, and this result qualitatively compares well with the experimental results (Tan *et al.* 1995).

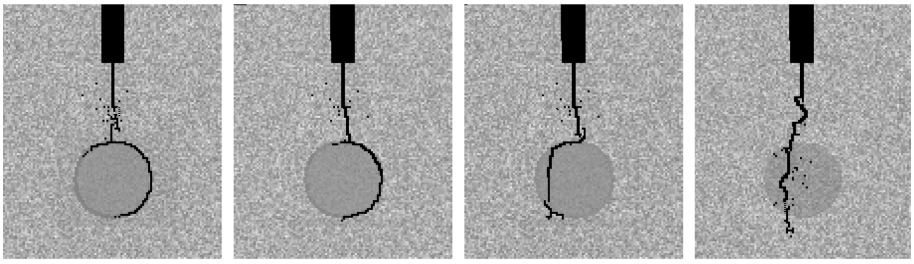

r = 0.4 r = 0.6 r = 0.8 r = 1.0

Fig. 8 Final cracking patterns of weak aggregate concrete with different mechanical parameters of bond phase (The ratio of mechanical parameters between bond phase and aggregate phase is denoted with *r*.)

4. Concrete specimen with multiple aggregates

In above numerical simulation, only an aggregate is included in the numerical specimen of concrete in order to quantify its effect on the macroscopic behavior of concrete subjected to tensile stress conditions. This specimen is far beyond the real concrete specimen experimented in the laboratory. However, it is the advantage of MFPA to include the heterogeneous structure of concrete

Table 2 Weibull distribution parameters of three concrete specimens subjected to uniaxial compression

	Phase	Mean of Young's modulus (GPa)	Mean of uniaxial compressive strength (MPa)	Homogeneity index *m*
Specimen I	Matrix	27.3	165	3.0
	Aggregate	80.0	500	6.0
	Bond	**11.44**	**70**	**3.0**
Specimen II	Matrix	27.3	165	3.0
	Aggregate	80.0	500	6.0
	Bond	**16.38**	**99**	**3.0**
Specimen III	Matrix	27.3	165	3.0
	Aggregate	80.0	500	6.0
	Bond	**15**	**150**	**1.5**

at the mesoscopic level in our numerical specimen.

In this section, three numerical specimens of concrete that consists in many aggregates with different size are numerically formed. In these numerical specimens, the Weibull distribution parameters are specified according the values listed in Table 2. For Specimen I and Specimen II, the ratio between mechanical properties of bond phase and matrix phase are 0.42 and 0.60, respectively. The volume ratio of the aggregate of the numerical specimen is 40%.

In order to simulate the constraint effect of loading platen on concrete specimen, two loading plate, which possesses the mechanical properties of steel (with a Young's modulus of 200 GPa, a uniaxial compressive strength of 400 MPa and a Poisson's ratio of 2.0) are also included in the numerical specimens (as shown in Fig. 11). To simulate the complete fracture process of a concrete specimen under uniaxial compression, the analysis was conducted with displacement control. That is, the load was applied through imposed displacements at one end, while the other end was prevented form vertical movement.

Fig. 9 shows the stress-strain curves of three specimens of concrete subjected to uniaxial compression. For Specimen I and II, their post-peak stress-strain curves are much more brittle,

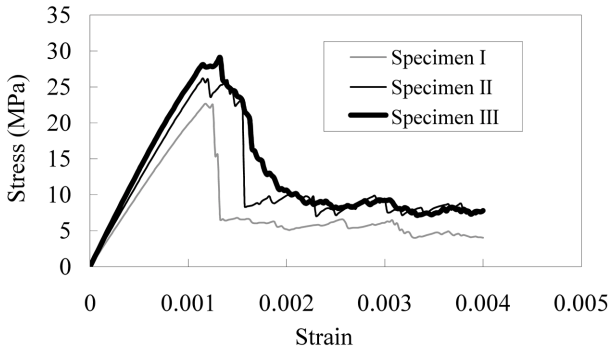

Fig. 9 Numerical results of axial stress-strain curves of Specimen I, Specimen II and Specimen III (The different mechanical parameters of bond phase are specified to these three specimens.)

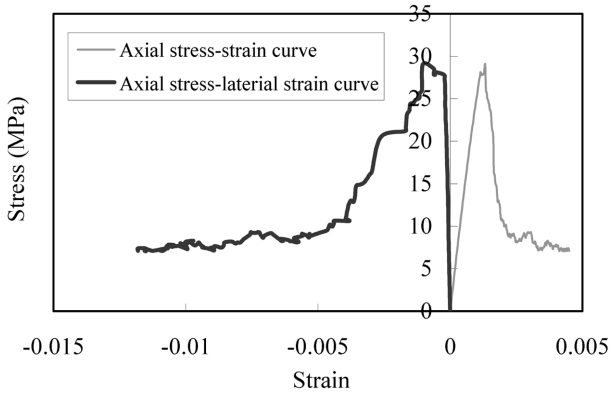

Fig. 10 Axial stress-strain curve and axial stress-lateral strain curve of Specimen III under uniaxial compression (numerical results)

which are quite different from those observed in laboratory test of normal strength concrete. In order to make the stress-strain response of concrete specimen is much similar that observed in laboratory test, the Weibull distribution parameters bond phase are suitably selected for Specimen III and are also listed in Table 2 based on to many numerical simulations of this kinds.

Fig. 10 shows the axial stress-axial strain curve, together with the axial stress-lateral strain curve of the Specimen III. The compressive strength and the elastic modulus of this numerical specimen are 30.0 MPa and 25.2 GPa respectively. The stress-strain curve has a shape that is similar to that observed in many laboratory experiments, with an ascending branch, a peak, which is commonly referred to as the compressive strength, and a descending branch or softening branch. The lateral strain is seen to show large increases in the post-peak region due to the onset of many cracks in the concrete. This phenomenon has been commonly observed in uniaxial compression tests of concrete. From the results of this numerical specimen, it can conclude that the very large lateral deformation and volume dilatancy of concrete can be simulated effectively by the present model.

In Fig. 11, the cracking patterns and maximum shear stress distribution during the fracture process of Specimen III are presented. In Fig. 11(a), the brightness of gray degree indicates the relative magnitude of elastic modulus of mesoscopic elements. The brighter the color is, the higher the value of Young's modulus of mesoscopic element is. The damage of elements will cause degradation of their elastic modulus and the elements totally damaged in tensile mode will be displayed as black color, thereafter, the cracking patterns of the concrete specimen during the complete fracture process can be seen from this figure. As shown in Fig. 11(b), the brightness in the maximum tensile stress figures indicates the magnitude of maximum tensile stress. The mesoscopic elements with higher maximum tensile stress damage preferentially in tensile mode.

Because the heterogeneity of concrete is incorporated in the numerical model, the stress state in the numerical specimen varies from one element to another. It can be seen that the many mesoscopic elements damage at the bond phase. These damaged elements subsequently induce stress concentrations around them, causing tensile damage in the adjacent elements. Therefore, the mechanical properties of bond phase have a significant effect on the initial cracking in the concrete, and therefore, it will affect the strength of concrete. At higher stress levels, the damaged elements will merge with each other by spreading through the matrix, with damage localised in small zones. At this point, a large number of elements are damaged in the tensile mode at the same time, and a

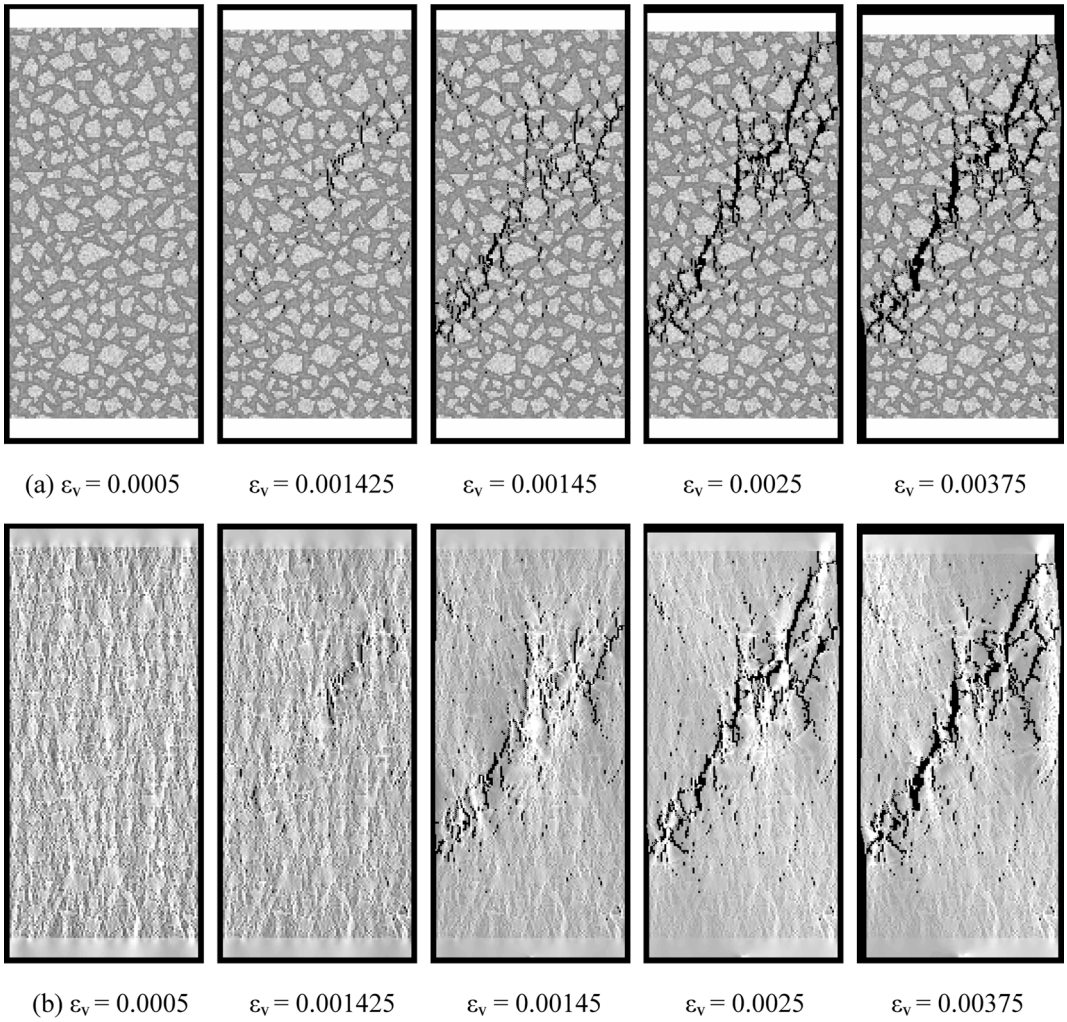

Fig. 11 Numerical results of fracture process of Specimen III subjected to uniaxial compression: (a) cracking patterns; (b) distribution of maximum shear stress (In this figure, ε_v denotes the axial strain, and ε_v is 0.001325 at the peak stress.)

great amount of strain energy is released, leading to a sharp decrease of the load-carrying capacity of the concrete. Finally, the damaged zones grow further in the matrix to surround the aggregate and to form macroscopic cracks. This failure pattern is similar to the experimental results of normal strength concrete obtained by Van Mier (1997) as well as Kupfer and Gerstle (1973). Many phenomena such as strain localization, stress redistribution and crack propagation process observed during the fracture process of concrete can be vividly captured with the numerical model used in this paper. It also proves that it is reasonable to study the concrete as a three-phase composite at the mesoscopic level in order to study its macroscopic mechanical response.

5. Conclusions

In this investigation, a numerical code named MFPA is used to study the influence of mesoscopic structures on the macroscopic strength and fracture characteristics based on that the concrete is assumed to be a three-phase composite composed of matrix (mortar), aggregate and bond between them. The following conclusions can be drawn:

(1) The mechanical parameters of bond phase have a significant effect on the crack propagation path in concrete, and, therefore, it has a significant effect on the macroscopic mechanical properties of concrete.

(2) For normal concrete under uniaxial compression, the mechanical properties of bond phase play an important role in macroscopic response of concrete. The non-linearity of the stress-strain curve is mainly dominated by the mechanical properties of bond phase. The whole fracture process of concrete specimen can be reproduced well with MFPA by choosing the suitable parameters of three phases of concrete.

(3) Many phenomena such as strain localization, stress redistribution and crack propagation process observed during the fracture process of concrete can be vividly captured with the numerical model. Such a modelling approach can offer a helpful tool for studying the mechanical performance of concrete with heterogeneous mesoscopic structures and mechanical parameters.

Acknowledgements

This work presented in this report is supported by the Liaoning Provincial Natural Science Foundation (Grant No.20031019) of P.R. China. The authors are grateful for this support.

References

Bažant, Z.P., Tabbara, M.R., Kazemi, M.T. and Pijaudier-Cabot, G. (1990), "Random particle model for fracture of aggregate or fiber composites", *J. Eng. Mech.*, ASCE, **116**(8), 1686-1705.

Kupfer, H.B. and Gerstle, K.H. (1973), "Behavior of concrete under biaxial stresses", *J. Eng. Mech. Div.*, ASCE, **99**(EM4), 852-866.

Mohamed, A.R. and Hansen, W. (1999a), "Micromechanical modeling of concrete response under static loading ---- Part I: Model development and validation", *ACI Mater. J.*, **96**(2), 196-203.

Mohamed, A.R. and Hansen, W. (1999b), "Micromechanical modeling of crack-aggregate interaction in concrete materials", *Cement and Concrete Composites*, **21**, 349-359.

Pearce, C.J., Thavalingam, A., Liao, Z. and Bićanić, N. (2000), "Computational aspects of the discontinuous deformation analysis framework for modeling concrete fracture", *Engineering Fracture Mechanics*, **65**, 283-298.

Schangen, E. and Van Mier, J.G.M. (1992), "Experimental and numerical analysis of micromechanisms of fracture of cement-based composites", *Cement and Concrete Composites*, **14**, 105-118.

Tan, D.M., Tschegg, E.K., Rotter, H. and Krinchner, H.O.K. (1995), "Cracks at mortar-stone interfaces", *Acta Mettallurgica*, **43**(10), 3701-3707.

Tang, C.A. (1997), "Numerical simulation on progressive failure leading to collapse and associated seismicity", *Int. J. of Rock Mechanics and Mining Science*, **34**(2), 249-261.

Tang, C.A., Liu, H., Lee, P.K.K., Tsui, Y. and Tham, L.G. (2002), "Numerical studies of the influence of

microstructure on rock failure in uniaxial compression, Part I: Effect of heterogeneity", *Int. J. of Rock Mechanics and Mining Science*, **37**, 555-569.

Van Mier, J.G.M. (1997), *Fracture Processes of Concrete: Assessment of Material Parameters for Fracture Models*. Boca Raton, Florida: CRC Press, Inc.

Van Mier, J.G.M. and Van Vliet, M.R.A. (1999), "Experimentation, numerical simulation and the role of engineering judgement in the fracture mechanics of concrete and concrete structures", *Construction and Building Materials*, **13**, 3-14.

Vonk, R.A., Rutten, H.S., Van Mier, J.G.M. and Fijneman, H.J. (1991), "Micromechanical simulation of concrete softening", In: Van Mier, J.G.M., Rots, J.G., Bakker, A.R., editors. *Proc. of the Int. RILEM/ESIS Conf., Fracture Processes in Concrete, Rock and Ceramics*. 2-6 Boundary Row, London: E. & F.N. Spon., 129-138.

Wittmann, F.H. (1983), "Structure of concrete with respect to crack formation", In: Wittmann, F.H. editor. *Fracture Mechanics of Concrete*. London/New York: Elsevier, 43-74.

Zhu, W.C., Teng, J.G. and Tang, C.A. (2002), "Numerical simulation of strength envelope and fracture patterns of concrete under biaxial Loading", *Magazine of Concrete Research*, **54**(6), 395-409.

Notation

The following symbols are used in this paper:

D^+	: damage variable for tensile damage;
D^-	: damage variable for shear damage;
E, E_0	: damaged and undamaged (initial) elastic modulus of element;
f_{c0}, f_{t0}	: compressive and tensile strengths of element respectively;
$f(u)$	: probability density function of Weibull distribution;
m	: homogeneity index, shape parameter of Weibull distribution;
r	: the ratio of mechanical parameters between bond and matrix phases in concrete;
u	: parameter of elements that conforms to Weibull distribution, such as elastic modulus and strength;
u_0	: scale parameter of Weibull distribution;
ε	: strain;
ε_0	: strain at peak stress of specimen;
ε_1, ε_2, ε_3	: principal strain;
ε_{c0}	: strain at the peak compressive stress;
ε_{t0}	: strain at the peak tensile stress;
ε_{tu}	: ultimate tensile strain;
ϕ	: internal friction angle;
η	: ultimate tensile strain coefficient;
λ	: residual strength coefficient;
μ	: Poisson's ratio;
σ	: stress;
σ_1, σ_2, σ_3	: principal stress